

ARTICLES

Synchronous Growth of Vertically Aligned Carbon Nanotubes with Pristine Stress in the Heterogeneous Catalysis Process**Qiang Zhang, Weiping Zhou, Weizhong Qian, Rong Xiang, Jiaqi Huang, Dezheng Wang, and Fei Wei****Beijing Key Laboratory of Green Chemical Reaction Engineering and Technology, Department of Chemical Engineering, Tsinghua University, Beijing 100084, China**Received: April 26, 2007; In Final Form: August 4, 2007*

The formation of a vertically aligned carbon nanotube (VA-CNT) array in a floating catalyst process was described as a synchronous growth that resulted from the interaction of fast growth and slow growth CNTs. The array growth was characterized by the observations that straight and curved CNTs were formed during growth, and the tortuosity change of the curved CNTs and a G band Raman shift during growth. These were used to deduce that pristine stress was present in the CNTs. A model of the stresses as caused by space limitation and different growth rates was used to explain the development of a synchronous growth of the VA-CNT array. The tortuosity of the curved CNTs and Raman shift decreased and were constant after the growth of a certain length of the array, indicating that constant stresses were maintained in the growing array after the growth of this length. This indicated that an ordered CNT structure was formed and a transition from random structure to ordered structure growth had taken place in the growth. The transition was explained by a thermodynamic argument using the Onsager virial theory. Based on the vapor–liquid–solid model and bottom up growth for a single CNT, the description of a synchronous growth made possible by existent stresses gives a view that accounts for the interaction between CNTs in an array, and it can provide guidelines for a more precise control of the array structure.

Introduction

Since the first synthesis in 1996,¹ vertically aligned carbon nanotube (CNT) arrays have become one focus of research in nanoscience and nanoengineering. These aligned CNTs in array form have many attractive properties, such as identical tube length, uniform orientation, extra high purity, easy spinning into macroscopic fibers, etc. As-grown arrays can be used directly to construct field emission devices, anisotropic conductive materials, multi-functional membranes, and super strong yarn.^{2–4} Even after the loss of the original alignment, longer and straighter multiwalled CNTs (MWCNTs) from the CNT arrays were better than randomly aggregated multiwalled or even single-walled CNTs (SWCNTs) in improving the electronic, mechanic, and thermal properties of polymers.⁵ These applications can become widespread if a controllable synthesis of CNT arrays at a low cost in a scalable way can be developed. Various synthesis methods have been developed, which include porosity assisted chemical vapor deposition (CVD),¹ plasma enhanced CVD,⁶ thermal CVD,^{7,8} alcohol feed CVD,⁹ and floating catalyst CVD.^{10–14} Among these, the floating catalyst process has the advantages of not needing prior catalyst preparation, easily controllable synthesis, simple apparatus, low cost, and is easily scalable.^{10,12}

During the synthesis of CNT arrays by the floating catalyst process, the array growth mechanism is still not understood.

Until now, research on CNT growth mechanism has been mainly on the atomic scale, for example, the vapor–liquid–solid (VLS) model. The VLS model explains how a single CNT grows from the catalyst,^{15,16} but gives little information about how CNTs can grow into an array morphology. Recently, the growth site of an array was indicated to be at the bottom of the array. This mechanism, which was confirmed by catalyst labeling and multilayer growth observations,^{17–20} gave the growth direction of single CNT and informed us of the importance of maintaining the catalyst and carbon source at the bottom of the CNT array, but indicated little about the formation of the array. There have been many reports on catalyst nucleation and array growth with the VLS model in plasma enhanced CVD^{21–23} and thermal CVD on a wafer.²⁴ There are now also some reports that have increased our understanding of surface diffusion and the reaction rate of CNT array formation.²⁵ Yet there are few reports on the interaction of the CNTs in the array growth process.

CNT arrays grown with the floating catalyst process generally show synchronous growth. Hart and Slocum²⁶ have shown that an external stress in a thermal CVD process has a large effect on the structure of the CNTs in an array, but the basic morphology of the array was similar to that of CNT arrays grown in the absence of an external stress.^{10–14} This suggested that stresses might be present in the CNT array itself, which presumably is due to the interactions among the CNTs, and the details of this can be useful information. Also, a basic question in CNT array growth is why and how the CNTs form an ordered

* To whom correspondence may be addressed. Tel.: +86-10-62785464. Fax: +86-10-62772051. E-mail: weifei@flotu.org.

self-assembled structure, especially when beginning from an initial random structure. Increased understanding on this issue will help in acquiring better and precise control of the length and density of the CNT array, which has many potential applications.^{2–5}

In this Article, the morphology of multilayer CNT arrays grown by the floating catalyst process is analyzed. The change in the curvature of the CNTs and a Raman shift during growth were measured and used to characterize the presence of stress in the CNTs. An array growth that was synchronized by this pristine stress was proposed to describe the CNT array growth. Using the picture of synchronous growth in the presence of stress, the transition of the morphology of the array during growth from a random structure to an ordered structure was explained by thermodynamics with the Onsager viral theory.

Experimental Methods

The CNT arrays were grown on silica by the floating catalyst method using ferrocene as the catalyst precursor and cyclohexane as the solvent and carbon source. The concentration of the catalyst precursor in cyclohexane was 20 g/L. A quartz flake was placed in the center of a horizontal quartz tube with an inner diameter of 30 mm and length of 1200 mm as the growth substrate. The cyclohexane solution at a feed rate of 5 mL/h was injected by a motorized syringe pump into a carrier gas of 90% Ar and 10% H₂ at a flow rate of 600 mL/min into the reactor. The carbon source was decomposed by in situ formed metal catalyst at 800 °C. Specifically, we used an interim reactant supply method, instead of the oxidation gas etching method,^{17,18} to form a multilayer array. This method grows the CNT array by layers, and information on the top and bottom structure of each layer can be acquired by high-resolution scanning electron microscopy (HRSEM) observation. Thus, growth information and a precise morphology analysis of the as-grown CNT array can be obtained.

After the experiments, the product was taken out of the reactor and peeled from the substrate. HRSEM (JSM 7401F, at 5.0 kV) was used to characterize the morphology of the CNT arrays. High-resolution transmission electron microscopy (HRTEM, JEM 2010, at 120.0 kV) was used to observe the detailed structure of the CNT arrays. Raman spectroscopy of the CNTs was performed using a Raman microscope (Renishaw, RM2000, He–Ne laser excitation line 633.0 nm).

Results and Discussion

Unlike most heterogeneous reactions on a catalyst particle surface, the CNT array is a product that gives a record of its growth history. The CNT array synthesis was performed as a four-step interim reactant supply reaction with reaction steps of 15, 25, 40, and 40 min to produce a four-layer CNT array with a total length of 4.5 mm. The lengths of the layers were 520, 900, 1545, and 1568 μm , respectively (Figure 1a). The SEM images (Figure 1b–d) showed that the surface of the top array comprised two layers with an interface of Fe nanoparticles coated with carbon about 60 nm in diameter. Above the interface, there were twisted CNTs with no fixed orientation, which were formed by a surface reaction on the CNT array during array growth. The main CNT array was under this catalyst layer, with one fraction of the array being connected to the interface layer and comprising mainly straight CNTs. These were bunched together in patches and comprised the straight fraction of the array. Another fraction of the CNT array comprised curved CNTs (Figure 1c,e,f). The curvature of the curved CNTs can change and will be discussed later. These

two fractions will be called Type 1 (straight, the arrow pointed CNTs in Figure 1c,e,f and Figure S1) and Type 2 (curved) CNTs, respectively.

Figure 1d,g,h, and Figure S2a,b show that the top of the array had a woven structure similar to the top crust of entangled nanotubes on the SWCNT arrays of Zhang et al.²⁴ In the woven structure, most of the tubes were connected to the main array, but tiny single thin-walled tubes were also found (Figure 1h). At the bottom of the array (Figure 1i,j, Figure S2c,d), several tubes formed a bundle that had a tiny thin tube wound around them (Figure 1j). From the contrast caused by backscattering electrons shown in Figure 1j, it can be deduced that most of the CNTs had catalysts at the bottom ends; that is, there were active catalysts at the bottom. This confirmed the root growth mode for the CNTs in the array.^{17–20} The root growth mode was corroborated by the differences in lengths with different growth times of each layer. In agreement with most reported results,^{10–14,27–29} the array did not contain very straight tubes, and there were complicated connections at the ends. As shown in Figure 2a, the CNT array growth rate from cyclohexane was that of rapid growth.^{11,29} The woven structure can be modulated by substrate size^{2,30} and formation time.³⁰

The Raman spectra were taken with a 20 μm^2 area sample at various locations along the CNT array and provided an averaged result. The G bands as a function of the growth length are shown in Figure 2b. These were shifted, with different shifts that gradually increased with array growth. The Raman band shift reached a constant value after 40 μm length of array growth.

The curvature of the Type 2 CNTs was quantitatively described by a tortuosity factor (Figure 2d) defined as the ratio of the length of the curved line between two points (blue line in Figure 2d) to linear distance between the two points (red line in the Figure 2d) using a method similar to that used by Zhou et al.³¹ The tortuosity factor is based on the dimensions of the CNT and has a higher resolution than small-angle X-ray scattering for the quantitative characterization of the curvature of the CNTs in the array. The tortuosity factor of each of the layers showed the same trend and decreased to a constant value after they reached a (straight) length of 160 μm (Figure 2d) where the curved CNTs began to show self-organization gradually. This length is slightly different from the length where the Raman shift became constant. The CNT alignment got better with increased CNT length. A transition to when an ordered structure was formed is shown in Figure 1c–f and Figure 2c,d.

This discussion will take as the basic observation that there were curved (Type 2) CNTs in the array, shown in Figure 1d, that did not directly comprise the woven structure, which indicated that Type 2 CNTs were formed after the formation of the woven structure. Type 1 CNTs are those that were grown first to comprise the woven structure, which eventually formed the straight CNTs connected to the woven structure and the array bottom shown in Figure 1c, e, and f. It is suggested that this situation was due to that the floating catalyst method resulted in catalyst particles of different sizes with different activities for CNT growth, and this gave rise to different CNT growth rates. Here, for the discussion, this will be simplified to two different growth rates: a fast growth that grew the Type 1 CNTs and the woven structure, and a slow growth that grew the Type 2 CNTs that had to grow under the woven structure.

The formation of the woven structure will be taken as given and we discuss the subsequent growth. From the existence of the woven structure, the picture can be suggested that the density of fast growth catalytic sites was low enough to prevent the Type 1 CNTs from being initially directed upward (perpen-

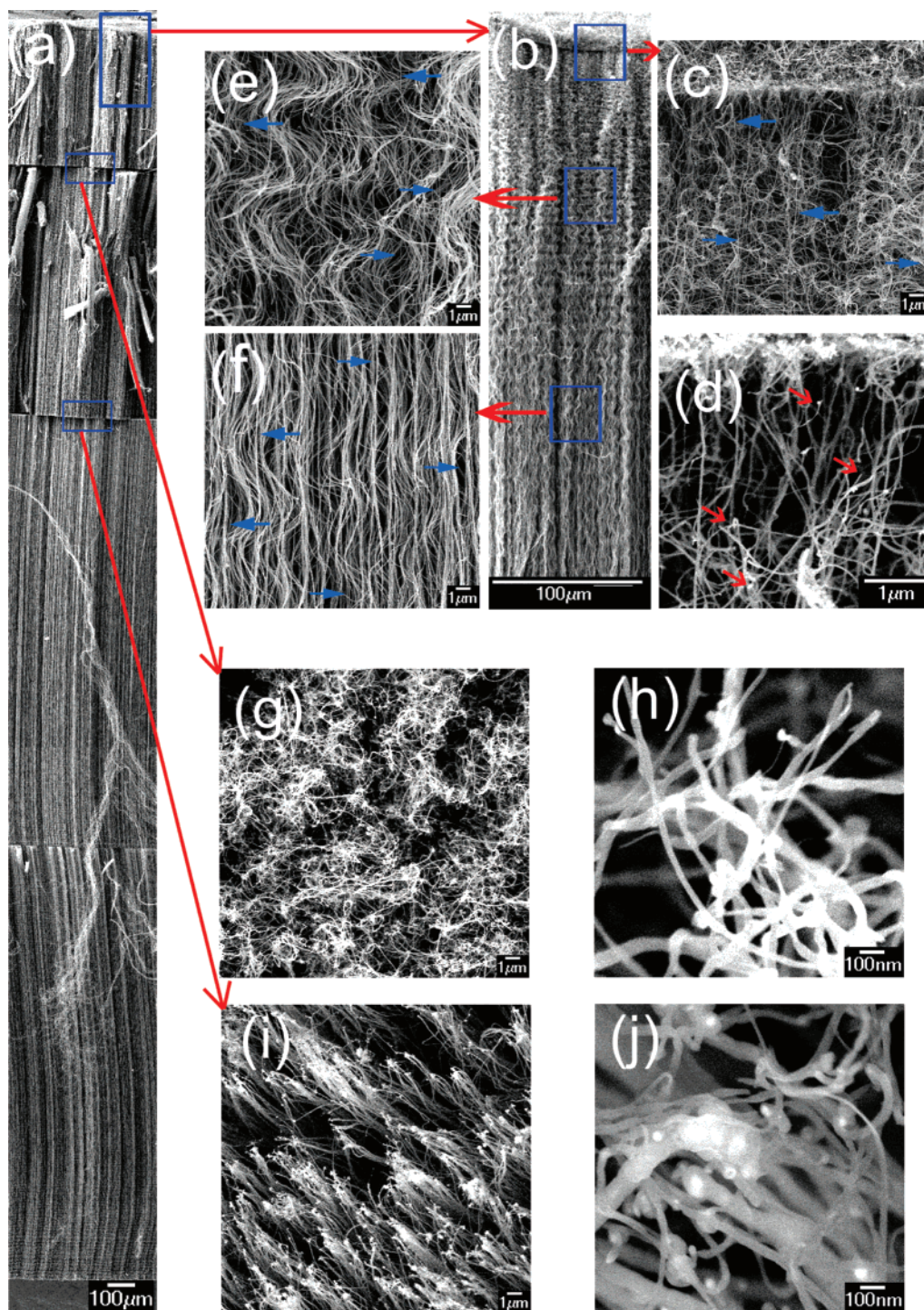


Figure 1. Morphology of the four-layer CNT array: (a) Overview of the CNT array, (b) cross section, (c) view of the top, (d) magnification of the first layer of the CNT array, (e) cross section at $60\ \mu\text{m}$ and (f) $360\ \mu\text{m}$ of the first layer; (g) low magnification and (h) high magnification of the top morphology of the second layer; (i) low magnification and (j) high magnification of the bottom morphology of the second layer. Type 1 (straight, the arrow pointed CNTs in Figure 1c,e,f) and Type 2 (curved) CNTs, which were related to synchronous growth, were shown in the CNT arrays.

dicular to the substrate) by being crowded, but was still high enough to cause entanglement between CNTs that grew the woven structure. It is now supposed that the catalytic sites were distributed randomly so that the slow growth catalytic sites were dispersed among the fast growth catalytic sites, and when growth began at the slow growth catalytic sites, their Type 2 CNTs grew directed upward due to crowding on the substrate. As these grew upward, they met space resistance to their growth at the woven structure. There will then be a stress on each Type 2 CNT due to this. In particular, there is a compressive stress on

the Type 2 CNTs against their growth upward due to the woven structure, and there is a tensile stress on the Type 1 CNTs comprising the woven structure due to the growing Type 2 CNTs pushing upward. The compression stress on the Type 2 CNTs was estimated to be about $5 \times 10^{-7}\ \text{N}$ from the critical buckling stress that curved a CNT.

The presence of curved Type 2 CNTs was one piece of evidence for the presence of pristine stress in the CNT array. This was corroborated by the change in their curvature with array growth (Figure 2d) and by the Raman shift shown in

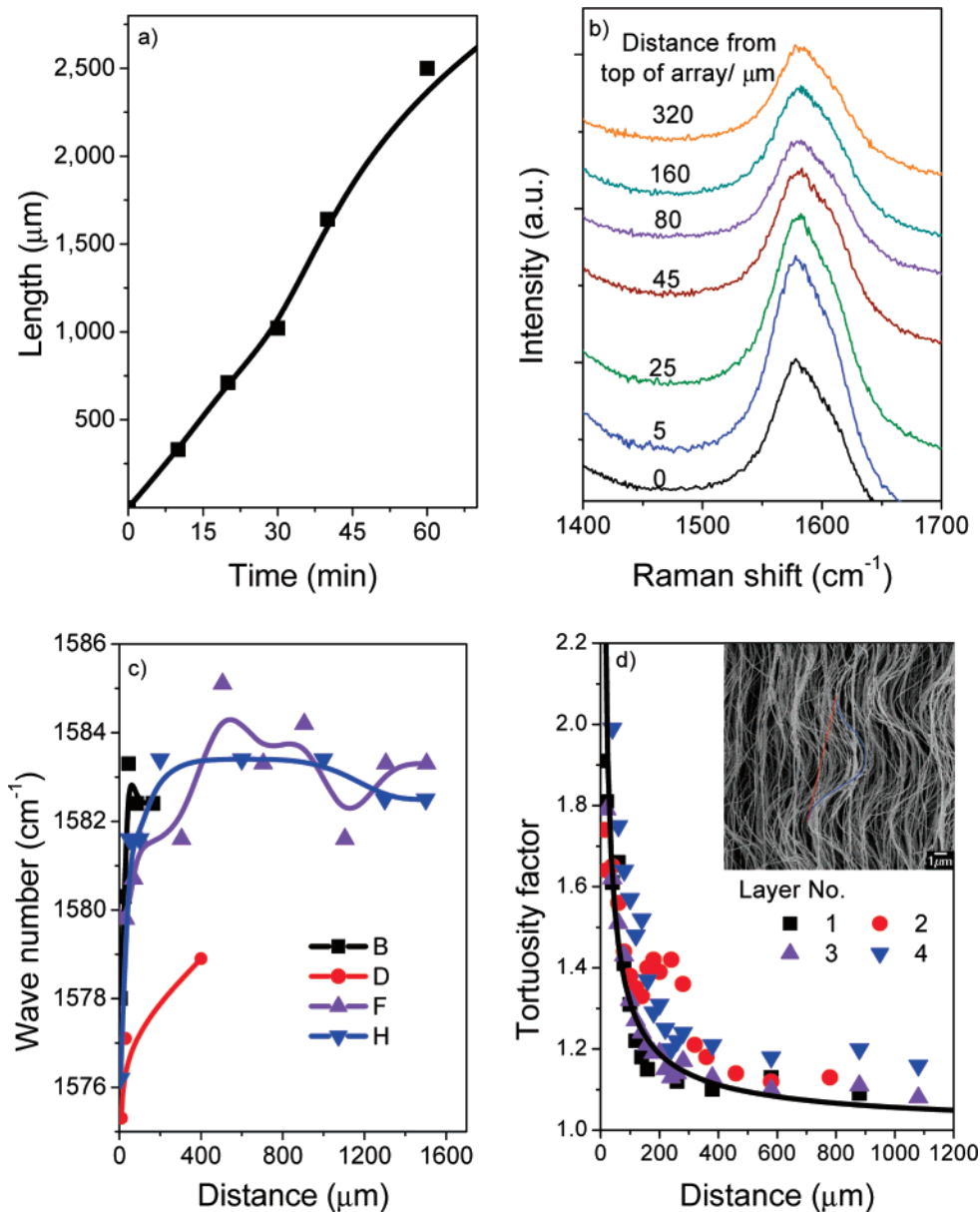


Figure 2. Quantitative description of the four-layer CNT array: (a) Growth rates in the floating catalyst process in the first hour, (b) Raman spectra of the first layer at different positions from the top, (c) Raman G band shift that corroborated the existence of stress in the array, and (d) tortuosity at different positions. The inset shows the measured tortuosity factor for the Type 2 (curved) CNTs defined as the length ratio of the blue to red lines.

Figure 2c, where the interpretation is used that a G band shift reflects the presence of stress in the CNT. A progressive shift toward higher frequency of the G band with increasing pressure on the CNTs is well documented.^{32–36} The shifts, which Merlen et al.³⁴ attributed to hardened carbon–carbon interactions, were observed with single walled CNTs and graphite and the application of high pressure, so the macroscopic physics is different from that in the CNT array here, but the notion that there is a similarity in that stress or lattice distortions exist in both cases is probably valid; that is, we can assume that a curved CNT has slightly different carbon–carbon interactions from that of a straight CNT. Although the assignment is not unequivocal (the shift can also be due to changing environment, e.g., more CNT bundles), the interpretation here is that the shifts reflect CNT stress or lattice distortions that change the frequency or relative intensities of the G component peaks.

The CNT array showed a synchronous growth explained as follows. Type 2 CNTs, which were originally unconnected to the woven structure, had a higher vertical growth rate when

they first began growing, but they had to grow into a curved structure due to the compressive stress imposed by space limitation by the woven structure. The tortuosity of Type 2 CNTs synchronized them to the array vertical growth. At the same time, the tensile stress on Type 1 CNTs imposed by Type 2 CNTs pulled the Type 1 CNTs into vertical growth, which synchronized them to the array vertical growth. Next, with more growth, the curved structure and random growth morphology during the initial growth was released gradually by synchronous growth and order alignment made possible due to the existent stresses in the array. The existence of these two kinds of CNTs and stresses in the CNT array was also confirmed by the direct measurement (Hysitron Triboscope with a Berkovich tip)^{37,38} of the mechanical property of the CNT array. Furthermore, such structures, like a mattress, show good energy absorption, and they have excellent mechanical properties as reported by Cao et al.³⁹

The transition to an ordered structure (Figure 1c–f and Figure 2c,d) is favored by thermodynamics as follows. The CNTs were

modeled as thin rod-like particles, and the thermodynamics state was described by the Onsager virial theory.⁴⁰ This theory predicts a phase transition from a random distribution to an order distribution above a transition value of D/vL , where D is the diameter of the rod-like particles, L is the length of the rod-like particles, and v is the volume concentration. When D/vL is smaller than 3.3, the random distribution is more stable, and vice versa above 4.8. When the CNTs were short, the random distribution was more stable (Figure 1c). After the CNTs had grown longer than a certain height, about 10 μm in our case from the Onsager virial theory, ordered structures were stable. Experimentally, the transition was observed after the array was about 160 μm (Figure 1f, Figure 2d, Figure S2, Figure S3). The difference may be because of the simple model and that the CNTs in the array were not thin rod-like particles. It can be noted that if the CNTs do not convert to an ordered structure, they will remain in a high stress state as they grow, which will be a high energy state. This is a thermodynamic reason for VA-CNT array growth in the floating catalyst process. This is perhaps the situation with CNTs grown from powder catalysts in that they have such a low length to one hundred micrometers with agglomerated state.^{41,42} In that situation, the condition for thermodynamic stability and the very limited space available lead to that, among the grown CNTs, the CNTs are always tangled together because the transition would occur at a much larger length than can occur.

From the above, we get the picture of the synchronous growth of a CNT array induced by stress in the floating catalyst process in Figure 3. Ferrocene introduced into the reactor decomposed into Fe atoms, clustered into Fe nanoparticles, and deposited on the substrate (Figure 3a), and CNTs began growing on these. At the beginning, catalyst particles were present in low density and CNTs grew randomly on the substrate. At the same time, new catalyst particles were formed and the CNTs grew longer (Figure 3b). When the CNTs exceeded a certain length, they entangled and formed a woven structure. Subsequently, the CNTs cannot grow freely on the surface due to the limited space in the horizontal and vertical direction: a compressive stress is placed on later formed Type 2 CNTs and a tensile stress placed on the weave-connected Type 1 CNTs (Figure 3c). The stress distributed between the CNTs in the array during growth kept the straight and curved CNTs growing at the same macroscopic rate. After 1.5 min weave formation to an array height of 40 μm , the stress reached a constant value (Figure 3d). Thus, a synchronous growth of CNT array with pristine stress occurred in the floating catalyst process. The curvature of Type 2 CNTs can be increased by an external force.²⁶ The curvatures of the CNTs varied with length and can be changed when the CNTs grow even longer in a super long CNT array from the floating catalyst process shown in the Supporting Information (Figure S4). This is consistent with the Wang et al.^{43,44} results that were based on vertically aligned CNT array and thermal CVD, and the reasons for these are the object of ongoing quantitative studies.

Finally, it can be pointed out that a synchronous growth of CNT array was not only found in the floating catalyst process, but also in other heterogeneous catalytically CVD processes. This is because pristine stress commonly exists during array growth with various methods; that is, similar CNT array structure obtained with different CVD methods was because the interaction among the CNTs in the array is the key factor for array formation. It may be related to the growth termination of super long CNT arrays. In the thermodynamic model, Onsager virial theory of structure change in the growth process,

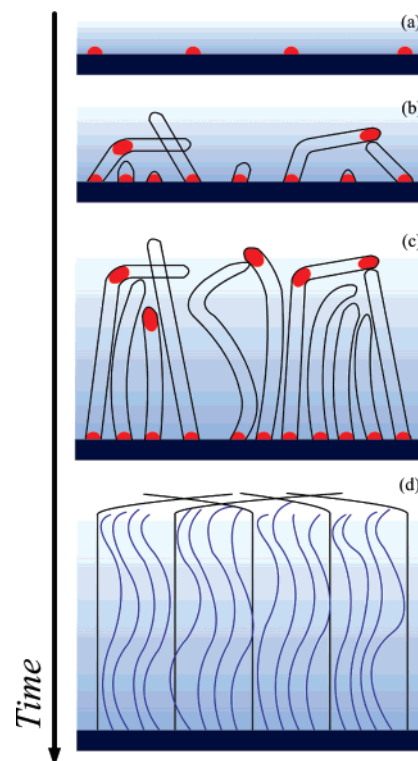


Figure 3. Schematic description of the synchronous growth of CNT array with pristine stress in the floating catalyst process: (a) Catalyst formation, (b) CNT nucleation and CNT random growth on the substrate and a woven structure formed after a period of growth, (c) CNTs now cannot grow freely on the surface due to horizontal and vertical resistance and stress created by the interactions between upward growing later formed Type 2 CNTs and the earlier formed Type 1 CNTs that comprised the woven structure. The stresses kept the straight and curved CNTs growing at the same macroscopic rate. (d) Synchronous growth of long CNT array with pristine stress, where the blue lines are Type 2 CNTs and the black lines are Type 1 CNTs that have the same vertical rate that is the overall (macroscopic) growth rate of the CNT array.

the catalyst density and formation rate are important factors. These are closely related to the volume and affect the formation of array structure according to the Onsager virial theory.

Conclusions

An interim reactant supply method in the floating catalyst process was used to produce a multilayer array growth. The CNT morphologies of the bottom, top, and cross-sections of the layers at various heights were determined. Based on the VSL model and root growth for single CNTs, an array growth due to the interactions between fast growth CNTs that developed a woven structure and later grown slow growth CNTs was proposed. The interactions led to the presence of pristine stress that led to synchronous growth. The presence of stress was corroborated by the presence of curved CNTs in the array, and the change in their curvature and a G band shift in the Raman spectra with growth. Two kinds of CNTs, curved and straight, were found. Thermodynamics and the Onsager virial theory were used to explain the structure transition from random to aligned growth.

Acknowledgment. The work was supported by the Foundation for the Author of National Excellent Doctoral Dissertation of PR China (No. 200548), Natural Scientific Foundation of China (No. 20606020), China National program (No. 2006CB932702), and Key Project of Chinese Ministry of

Education (No. 106011). We thank Prof. Quanshui Zheng for the helpful discussion.

Supporting Information Available: Estimated energies involved in formation of a single CNT, SEM images of a four-layer CNT array (Figures S1 and S2), TEM images of CNT array (Figure S3), and the morphologies of another super-long CNT array of 5.5 mm (Figure S4). This material is available free of charge via the Internet at <http://pubs.acs.org>.

References and Notes

- (1) Li, W. Z.; Xie, S. S.; Qian, L. X.; Chang, B. H.; Zou, B. S.; Zhou, W. Y.; Zhao, R. A.; Wang, G. *Science* **1996**, *274*, 1701–1703.
- (2) Cao, A. Y.; Veedu, V. P.; Li, X. S.; Yao, Z. L.; Ghasemi-Nejhad, M. N.; Ajayan, P. M. *Nat. Mater.* **2005**, *4*, 540–545.
- (3) Zhang, X. F.; Li, Q. W.; Tu, Y.; Li, Y.; Coulter, J. Y.; Zheng, L. X.; Zhao, Y. H.; Jia, Q. X.; Peterson, D. E.; Zhu, Y. T. *Small* **2007**, *3*, 244–248.
- (4) Li, X. S.; Zhu, G. Y.; Dordick, J. S.; Ajayan, P. M. *Small* **2007**, *3*, 595–599.
- (5) Moaisala, A.; Li, Q.; Kinloch, I. A.; Windle, A. H. *Compos. Sci. Technol.* **2006**, *66*, 1285–1288.
- (6) Ren, Z. F.; Huang, Z. P.; Xu, J. W.; Wang, J. H.; Bush, P.; Siegal, M. P.; Provencio, P. N. *Science* **1998**, *282*, 1105–1107.
- (7) Fan, S. S.; Chapline, M. G.; Franklin, N. R.; Tomblor, T. W.; Cassell, A. M.; Dai, H. J. *Science* **1999**, *283*, 512–514.
- (8) Hata, K.; Futaba, D. N.; Mizuno, K.; Namai, T.; Yumura, M.; Iijima, S. *Science* **2004**, *306*, 1362–1364.
- (9) Murakami, Y.; Chiashi, S.; Miyauchi, Y.; Hu, M. H.; Ogura, M.; Okubo, T.; Maruyama, S. *Chem. Phys. Lett.* **2004**, *385*, 298–303.
- (10) Andrews, R.; Jacques, D.; Rao, A. M.; Derbyshire, F.; Qian, D.; Fan, X.; Dickey, E. C.; Chen, J. *Chem. Phys. Lett.* **1999**, *303*, 467–474.
- (11) Zhang, X. F.; Cao, A. Y.; Wei, B. Q.; Li, Y. H.; Wei, J. Q.; Xu, C. L.; Wu, D. H. *Chem. Phys. Lett.* **2002**, *362*, 285–290.
- (12) Singh, C.; Shaffer, M. S. P.; Koziol, K. K. K.; Kinloch, I. A.; Windle, A. H. *Chem. Phys. Lett.* **2003**, *372*, 860–865.
- (13) Barreiro, A.; Selbmann, D.; Pichler, T.; Biedermann, K.; Gemming, T.; Rummeli, M. H.; Schwalke, U.; Buchner, B. *Appl. Phys., A* **2006**, *82*, 719–725.
- (14) Liu, J.; Webster, S.; Carroll, D. L. *Appl. Phys. Lett.* **2006**, *88*, 213119.
- (15) Kukovitsky, E. F.; L'vov, S. G.; Sainov, N. A. *Chem. Phys. Lett.* **2000**, *317*, 65–70.
- (16) Qian, W. Z.; Wei, F.; Liu, T.; Wang, Z. W.; Li, Y. D. *J. Chem. Phys.* **2003**, *118*, 878–882.
- (17) Li, X. S.; Cao, A. Y.; Jung, Y. J.; Wajtai, R.; Ajayan, P. M. *Nano Lett.* **2005**, *5*, 1997–2000.
- (18) Zhu, L. B.; Xu, J. W.; Xiao, F.; Jiang, H. J.; Hess, D. W.; Wong, C. P. *Carbon* **2007**, *45*, 344–348.
- (19) Iwasaki, T.; Zhong, G. F.; Aikawa, T.; Yoshida, T.; Kawarada, H. *J. Phys. Chem. B* **2005**, *109*, 19556–19559.
- (20) Xiang, R.; Luo, G. H.; Qian, W. Z.; Zhang, Q.; Wang, Y.; Wei, F.; Li, Q.; Cao, A. Y. *Adv. Mater.* **2007**, *19*, 2360–2363.
- (21) Merkulov, V. I.; Lowndes, D. H.; Wei, Y. Y.; Eres, G.; Voelkl, E. *Appl. Phys. Lett.* **2000**, *76*, 3555–3557.
- (22) Bower, C.; Zhou, O.; Zhu, W.; Werder, D. J.; Jin, S. *Appl. Phys. Lett.* **2000**, *77*, 2767–2769.
- (23) Merkulov, V. I.; Melechko, A. V.; Guillorn, M. A.; Lowndes, D. H.; Simpson, M. L. *Appl. Phys. Lett.* **2001**, *79*, 2970–2972.
- (24) Zhang, L.; Li, Z. J.; Tan, Y. Q.; Lolli, G.; Sakulchaicharoen, N.; Requejo, F. G.; Mun, B. S.; Resasco, D. E. *Chem. Mater.* **2006**, *18*, 5624–5629.
- (25) Louchev, O. A.; Laude, T.; Sato, Y.; Kanda, H. *J. Chem. Phys.* **2003**, *118*, 7622–7634.
- (26) Hart, A. J.; Slocum, A. H. *Nano Lett.* **2006**, *6*, 1254–1260.
- (27) Zhang, X. F.; Cao, A. Y.; Li, Y. H.; Xu, C. L.; Liang, J.; Wu, D. H.; Wei, B. Q. *Chem. Phys. Lett.* **2002**, *351*, 183–188.
- (28) Cao, A. Y.; Zhang, X. F.; Xu, C. L.; Liang, J.; Wu, D. H.; Wei, B. Q. *Appl. Surf. Sci.* **2001**, *181*, 234–238.
- (29) Singh, C.; Shaffer, M. S. P.; Windle, A. H. *Carbon* **2003**, *41*, 359–368.
- (30) Hart, A. J.; Slocum, A. H. *J. Phys. Chem. B* **2006**, *110*, 8250–8257.
- (31) Zhou, W. P.; Wu, Y. L.; Wei, F.; Luo, G. H.; Qian, W. Z. *Polymer* **2005**, *46*, 12689–12695.
- (32) Thomsen, C.; Reich, S.; Jantoljak, H.; Loa, I.; Syassen, K.; Burghard, M.; Duesberg, G. S.; Roth, S. *Appl. Phys., A* **1999**, *69*, 309–312.
- (33) Loa, I. *J. Raman Spectrosc.* **2003**, *34*, 611–627.
- (34) Merlen, A.; Bendiab, N.; Toulemonde, P.; Aouizerat, A.; San Miguel, A.; Sauvajol, J. L.; Montagnac, G.; Cardon, H.; Petit, P. *Phys. Rev. B* **2005**, *72*, 35409.
- (35) Wood, J. R.; Zhao, Q.; Wagner, H. D. *Composites, Part A* **2001**, *32*, 391–399.
- (36) Hadjiev, V. G.; Iliev, M. N.; Arepalli, S.; Nikolaev, P. *Appl. Phys. Lett.* **2001**, *78*, 3193–3195.
- (37) McCarter, C. M.; Richards, R. F.; Mesarovic, S. Dj.; Richards, C. D.; Bahr, D. F.; McClain, D.; Jiao, J. J. *Mater. Sci.* **2006**, *41*, 7872–7878.
- (38) Mesarovic, S. Dj.; McCarter, C. M.; Bahr, D. F.; Radhakrishnan, H.; Richards, R. F.; Richards, C. D.; McClain, D.; Jiao, J. *Scr. Mater.* **2007**, *56*, 157–160.
- (39) Cao, A. Y.; Dickrell, P. L.; Sawyer, W. G.; Ghasemi-Nejhad, M. N.; Ajayan, P. M. *Science* **2005**, *310*, 1307–1310.
- (40) Vroege, G. J.; Lekkerkerker, H. N. W. *Rep. Prog. Phys.* **1992**, *55*, 1241–1309.
- (41) Wang, Y.; Wei, F.; Luo, G. H.; Yu, H.; Gu, G. S. *Chem. Phys. Lett.* **2002**, *364*, 568–572.
- (42) Yu, H.; Zhang, Q. F.; Wei, F.; Qian, W. Z.; Luo, G. H. *Carbon* **2003**, *41*, 2939–2948.
- (43) Wang, H.; Xu, Z.; Eres, G. *Appl. Phys. Lett.* **2006**, *88*, 213111.
- (44) Wang, B. N.; Bennett, R. D.; Verploegen, E.; Hart, A. J.; Cohen, R. E. *J. Phys. Chem. C* **2007**, *111*, 5859–5865.